

## Kalman filter updating of rutting predictive models in flexible pavements using measured field data

Angela J. Haddad, George A. Saad & Ghassan R. Chehab

To cite this article: Angela J. Haddad, George A. Saad & Ghassan R. Chehab (2023) Kalman filter updating of rutting predictive models in flexible pavements using measured field data, International Journal of Pavement Engineering, 24:2, 2058700, DOI: [10.1080/10298436.2022.2058700](https://doi.org/10.1080/10298436.2022.2058700)

To link to this article: <https://doi.org/10.1080/10298436.2022.2058700>



Published online: 01 Apr 2022.



Submit your article to this journal [↗](#)



Article views: 180



View related articles [↗](#)



View Crossmark data [↗](#)

RESEARCH ARTICLE



# Kalman filter updating of rutting predictive models in flexible pavements using measured field data

Angela J. Haddad <sup>a</sup>, George A. Saad <sup>b</sup> and Ghassan R. Chehab <sup>c</sup>

<sup>a</sup>Department of Civil, Architectural and Environmental Engineering, The University of Texas at Austin; <sup>b</sup>Department of Civil and Environmental Engineering, American University of Beirut; <sup>c</sup>Department of Civil and Environmental Engineering, University of Illinois Urbana-Champaign

## ABSTRACT

Predicting pavement rutting is associated with significant uncertainties that often lead to inefficient maintenance planning. The predictive performance of rutting models is exacerbated in local road agencies and developing countries that rely on generic and knowledge-based models which are typically unreliable if used without adaptation, validation, or calibration. This study aims at developing a probabilistic framework that employs Ensemble Kalman Filter (EnKF) techniques to update the parameters associated with generic rutting predictive models while accounting for the prevailing uncertainties. When coupled with a continuous influx of measured data, the EnKF framework sequentially updates the generic models and minimizes prediction errors in real-time. The robustness of the presented scheme is demonstrated through a numerical example, and its sensitivity to the use of different generic curves as starting points is examined. The results indicate that the EnKF framework improves the accuracy of rutting predictions by up to 60% and that accuracy remains within tolerable limits whilst varying the range of the uncertainty in the measurements or the initial states. The paper concludes with a discussion of how practitioners can integrate the outcomes of the presented framework to enact maintenance policies that minimize the financial cost at the project and network levels.

## ARTICLE HISTORY

Received 28 August 2021  
Accepted 22 March 2022

## KEYWORDS

Asphalt pavement; rutting; Ensemble Kalman Filter; sequential data assimilation; pavement performance models; deterioration prediction

## 1. Introduction

With the growth in the global road network witnessed in the past decade, coupled with current and expected shortage in funding for infrastructure, transportation agencies are shifting their priorities from constructing new pavements to managing and maintaining existing networks (Xiong *et al.* 2012). Deterioration of the pavement structure of roadway networks is an expected phenomenon that roadway engineers plan and design for. While an asphalt pavement is typically designed to last for several decades, pavement conditions deteriorate much earlier than the design service life due to traffic, environment, material properties, and operational considerations (Underwood *et al.* 2017). Therefore, substantial investments are necessary to preserve, maintain, and extend the life of pavement networks (Pais *et al.* 2013; Gonzalo *et al.* 2018). However, due to the limited resource availability, it is critical to allocate budgets more effectively to satisfy pavement maintenance needs (TRIP 2016; ASCE 2017; Underwood *et al.* 2017). Consequently, pavement management systems (PMS) have received increasing attention as tools for supporting road agencies in making investment decisions and devising optimum maintenance strategies (AASHTO 2012; Pérez-Acebo *et al.* 2018). Deterioration models that forecast the progression of performance indicators, such as pavement distress and ride quality, are fundamental components of pavement management systems as they provide pavement managers with the necessary insights for timely maintenance interventions.

With the increase in traffic volumes, tire pressure, and axial loads in response to economic growth, rutting has become a prominent distress affecting asphalt pavements (Salama *et al.* 2006; Ekblad *et al.* 2021). Rutting is caused by the accumulation of permanent deformations or depressions along the wheel-path (White 2002). Base or subgrade rutting refers to the accumulation of permanent depressions in the unbound base or subgrade layer, while asphalt rutting denotes the permanent deformations located in the asphalt layer that are associated with densification and lateral upheavals (White 2002; ASTM, ASTM D6433-20 2020). The severity of pavement rutting is generally rated in terms of the rut depth which reflects the sum of subgrade, base, and asphalt rutting. Rutting primarily affects the safety and rideability of pavements since it could lead to vehicle hydroplaning and loss of skid resistance in wet weather, in addition to steering problems (Mamlouk *et al.* 2018). Therefore, pavements exhibiting rutting typically fail to maintain the necessary functional requirements long before achieving structural failure (Fwa *et al.* 2012).

The criticality of rutting to the safety of road users, coupled with its influence on pavement expenditure decisions, necessitates the development of highly accurate models that allow predicting the rate of increase in rutting depth, estimating the remaining pavement service life, and optimising road design and maintenance policies. To address the aforementioned need, this paper proposes a probabilistic framework that calibrates generic rutting models to minimise the mismatch between predicted and measured rut depths.

Specifically, this paper investigates using the Ensemble Kalman Filter (EnKF) paradigm to calibrate governing parameters of generic rutting propagation models using simple and non-costly rut depth measurements. The EnKF updating framework is applied to the generic family rutting models developed by Haddad et al (Haddad *et al.* 2021) and validated using rutting measurements obtained from the Long-term Pavement Performance database (LTPP). The presented methodology is of particular benefit to road agencies that are either applying their own PMS but do not have sufficient information to develop site-specific rutting prediction models or road agencies with established rutting family curves that require calibration for specific roads.

The rest of this paper is organised as follows. Section 2 provides a brief overview of the current state of pavement deterioration modelling, along with associated literature. Section 3 elaborates on the followed methodology by first discussing generic rutting deterioration models followed by the mathematical implementation details of the EnKF method within this study. Section 4 presents the model sensitivity analysis results and goodness of fit measures, along with a discussion of policy implications. Section 5 concludes the paper with a summary of the important findings, along with an identification of future research directions.

## 2. Background

In the current state of practice, rutting prediction models are either developed based on deterministic or probabilistic approaches. Several researchers and practitioners have worked on developing deterministic regression prediction models to simulate the progression of rutting, mostly using locally collected field data. Examples of these models include those developed by specific road agencies (George 2000; Choumanivong and Martin 2010; Wolters and Zimmerman 2010; Abu-Ennab 2015), the World Bank for the Highway Development and Management Model (HDM-4) (Jain *et al.* 2007; Pérez-Acebo *et al.* 2018), and the Mechanistic-Empirical Pavement Design Guide (AASHTO 2015). In addition to the traditional deterministic models that are available in the literature, researchers have also used neural network techniques to develop rutting prediction models (Yang *et al.* 2003; Thube 2012; Abambres and Ferreira 2018; Gong *et al.* 2018; Yao *et al.* 2019; Choi and Do 2020). Neural Network-based models introduced significant improvements to the performance of rutting models compared to the traditional ones. However, applying regression as well as neural network models is a challenging task as their predictive capacity relies heavily on detailed data regarding the road and environmental characteristics. Even with this information available, predictions are not always satisfactory because the models are intended to simulate rutting performance under a limited set of traffic and environmental conditions (Hjelle 2007; Jain *et al.* 2007; Von Quintus 2012; Bannour *et al.* 2019; Li *et al.* 2019). In addition to the latter challenges, the deterministic regression models provided in the literature are limited by their inability to capture the uncertainties underlying the rutting accumulation process. These uncertainties can be attributed to several sources including mathematical modelling simplifications,

non-homogeneity of materials, the stochastic nature of environmental and traffic conditions that vary spatially and temporally, and the inability to observe and quantify construction quality and variability (Zhang and Gao 2018).

In order to address the inherent uncertainties of the rutting deterioration process, probabilistic models have been developed (Jiménez and Mrawira 2012; Osorio-Lird *et al.* 2018; Pérez-Acebo *et al.* 2018; Yamany and Abraham 2021). Markov chain models are the most extensively used probabilistic models for forecasting pavement rutting (Amador-Jiménez and Mrawira 2012; Osorio-Lird *et al.* 2018; Wang *et al.* 2021; Yamany and Abraham 2021). Markovian models developed for predicting pavement rutting can be categorised into homogeneous, staged-homogeneous, and nonhomogeneous Markov models (Yamany and Abraham 2021). Several researchers have employed these techniques to predict rutting while accounting for uncertainties, such as those developed in (Pulugurta *et al.* 2013; Khan *et al.* 2014; Abaza 2016; Saha *et al.* 2017). However, Markov models do not explicitly consider the relationship between rutting and its causal factors rendering them inapplicable under traffic, environmental, and pavement material characteristics that are different from the ones they were originally created for (Jiménez and Mrawira 2012).

Based on the reviewed rutting prediction models, it is evident that the reliable implementation and development of all types of models are profoundly limited to the accurate identification and quantification of real site conditions and uncertainties. To that end, road agencies with well-developed PMS or those initiating pavement management systems collect pavement condition data on an ongoing basis (Zimmerman and Ram 2015; FHWA 2018). Additionally, AASHTO's Pavement Management Guide (AASHTO 2012) emphasises the importance of periodically reviewing the adopted models and updating them using the collected body of data to ensure the proper representation of the prevalent deterioration trends and the continuous improvement in the efficiency of the PMS (AASHTO 2012; Tabatabaee and Ziyadi 2013). AASHTO's Pavement Management Guide calibration methodologies range from simply 'shifting the curve' to intersect data points of interest to using Bayesian modelling techniques for incorporating field data into expert models (AASHTO 2012).

Bayesian approaches have been adopted by several researchers to perform model updates (Li *et al.* 1997; Hong and Prozzi 2006; Jiménez and Mrawira 2012; Luo *et al.* 2016; Haddad *et al.* 2021). In essence, Bayesian inference is a probabilistic approach that combines prior knowledge with observation to produce a newly adjusted probability of an event (Osorio-Lird *et al.* 2018). One of the earliest implementations of such frameworks was conducted by Li *et al.* to update the transition probability matrices used to predict deterioration using a Markov process (Li *et al.* 1997). Another implementation of Bayesian updating on Markov-based models was developed by Tabatabaee and Ziyadi using data collected from the Minnesota Department of Transportation test facility (Tabatabaee and Ziyadi 2013). An enhancement of the AASHTO deterioration model was also introduced through the application of a Bayesian updating approach (Hong and Prozzi 2006). Pavement performance based on the Bayesian approach was shown to be effective in estimating and updating

predictive models (Hong and Prozzi 2006). Park *et al.* also proposed a Bayesian based Kalman Filtering data analysis tool that provides a sound engineering and statistical framework for updating generic deterioration curves when road-specific data were obtained (Park *et al.* 2008). They demonstrated their framework on data collected by the Texas Transportation Institute at several sites in Texas to update a theoretical sigmoidal pavement distress equation with coefficients based on prior engineering knowledge. The results reveal that their Kalman filtering based Bayesian formulation gave compelling predictions as provided by the updated model parameters (Park *et al.* 2008). Jiménez and Mrawira presented a case study for updating Uzan's Rut Depth Model that originated in 1983 using data observations from the AASHTO Road Test (Jiménez and Mrawira 2012). Additionally, Luo *et al.* proposed a Bayesian approach to update design parameters of the fatigue and rutting mechanistic-empirical models that are available in the MEPDG (Luo *et al.* 2016). Inkoom *et al.* also demonstrated the efficiency of Bayesian modelling in accounting for the model uncertainty while predicting pavement deterioration using survival time data. The authors concluded that the posterior estimates obtained by updating generic survival curves using the Bayes theorem are accurate and that 95% of the observed survival times fall within the 95% posterior prediction intervals (Inkoom *et al.* 2020).

While the reviewed models demonstrated improvements in the prediction performance, to our knowledge, none of the presented approaches proposed a real-time update framework that continuously updates the used models whenever new observations become available. To overcome the deficiencies cited in the literature regarding the unreliability of generic and deterministic rutting models, this research aims to develop a probabilistic framework that uses the Ensemble Kalman filter (EnKF), a sequential data assimilation technique, to calibrate the governing parameters of generic rutting models by relying on actual field measurements. The calibrated models can then be utilised for simulating the rutting depth in flexible pavements and assessing the remaining service life to ultimately formulate maintenance decisions with higher reliability.

As mentioned earlier, the current study focuses on providing a practical and statistically robust method to improve and update rutting propagation predictions. It is generally assumed that transportation agencies start with generic family curves to perform performance predictions when no historical condition data are available. The coefficients of these generic models are typically based on expert knowledge and reflect the initial or prior belief about the deterioration process. The generic curves used to illustrate the methodology in this study are adopted from (Haddad *et al.* 2021). After rutting depth data is collected, the EnKF methodology is used to modify the initial prediction curve and its associated parameters to incorporate newly obtained measurement data. Data used to carry out the update process is obtained from rutting depth measurements collected from the LTPP.

### 3. Methodology

This section presents the methodology for implementing the EnKF framework for the scope and objectives of this research

study. This section starts with an overview of rutting depth prediction models then focuses on the family curves employed in this study. Later, general definitions of sequential data assimilation framework are presented, followed by the mathematical implementation of the EnKF framework in this study. The final component of this section combines the theory of the EnKF with the numerical example being considered in order to present how to apply EnKF for updating general rutting prediction models.

#### 3.1. Rutting depth prediction mathematical model

Pavement rutting refers to the accumulation of permanent strain in the pavement layers and occurs over three distinct phases. The first phase is referred to as the primary stage where the pavement undergoes rapid accumulation of permanent strain caused by volumetric changes resulting from densification. Initially, this phase starts with a high deformation rate that later decreases as the permanent deformation approaches the secondary stage (Zhou and Scullion 2002; AASHTO 2015). Volumetric changes continue in the secondary stage; however, they are accompanied by minimal shear deformations (Zhou and Scullion 2002; AASHTO 2015). In the tertiary stage, permanent deformation accumulates at an increasing rate, reflecting excessive shear deformations in the absence of volume reduction (Zhou and Scullion 2002; AASHTO 2015). The number of load repetitions to reach the tertiary zone is referred to as the tertiary rutting limit and it represents the cumulative traffic loading required for failure (Zhou and Scullion 2002; AASHTO 2015).

As mentioned previously, several general models are available in the literature to simulate the rutting mechanism; however, their applicability in developing countries and by road agencies with limited budgets and datasets remains challenging. Therefore, these entities typically rely on expert-based or generic family models that do not require extensive datasets or a large number of inputs to initiate their pavement management processes (Wolters and Zimmerman 2010; Saha *et al.* 2017). Expert or knowledge-based curves are generated by aggregating the knowledge of experienced engineers who are familiar with the local conditions; while, family curves are developed using data adopted from some roadway segments with similar traffic, climate, and pavement characteristics (Wolters and Zimmerman 2010; Saha *et al.* 2017).

Although generic models can be utilised in the absence of data, their main function is strictly limited to launching the pavement management system. Since such models include substantial inaccuracies due to the mathematical simplifications, they necessitate continuous calibration and updating whenever new rutting measurements are collected to achieve an adequate prediction accuracy. Since this study proposes an EnKF updating framework, a generic rutting prediction model is used to validate the application. It is worth noting that the model that will be used for numerical validation in this research presents a mere illustrative case study; alternatively, any other generic model can be incorporated.

The generic family curves adopted in this study were developed by Haddad *et al.* as part of a study to develop machine learning based models for pavement rutting prediction

(Haddad *et al.* 2021). The outcome of these efforts includes 27 family curves corresponding to various traffic, climate, and mix design combinations (Haddad *et al.* 2021). These curves were extracted from the outputs of a deep neural network model that was developed using a comprehensive dataset obtained from the Long-Term Pavement Performance (LTPP) database. The LTPP was established in 1991 by the Federal Highway Administration (FHWA) and it includes data corresponding to more than 2500 pavement sections located in North America (Baladi *et al.* 2017; Elkins *et al.* 2018). Its main purpose is to evaluate the long-term performance of pavements subject to different structural designs, materials, maintenance activities, traffic loads, and climatic conditions (Baladi *et al.* 2017).

### 3.2. Numerical application

The efficiency of the presented framework is illustrated using fourteen rutting measurements extracted from the LTPP corresponding to road section 112 in the State of Alabama (LTPP InfoPave *n.d.*). The selected road is a segment of an interstate lying in a wet non-freeze (WNF) climatic zone. Additionally, the associated pavement mix design results in a good rutting performance. As a result, the used generic rutting curve should reflect this example's specific traffic (*i.e.* interstate), climate (*i.e.* WNF), and mix design characteristics (*i.e.* high rutting resistance). Additional curves corresponding to other families are also used to investigate the sensitivity and robustness of the EnKF framework. Such an evaluation is essential since road agencies may not have sufficient information to select the appropriate family curve. Therefore, the framework is assessed using initial state vectors corresponding to three family curves as presented in Table 1 (Haddad *et al.* 2021). Table 1 presents three scenarios that were arbitrarily selected to showcase the proposed EnKF framework. Scenario 1 is a curve that belongs to the same family as road 112 in Alabama, Scenario 2 belong to the same climate zone but the mix has an inferior performance (*i.e.* Medium resistance), and Scenario 3 corresponds to a different climate zone and mix performance. Figure 1 shows a graphical illustration of the scenarios of Table 1 and indicates how far their predictions are from the actual rutting measurements. It is worthwhile to note that all the generic curves that are used to validate the EnKF framework have a mathematical structure of a third-degree polynomial where the rut depth (RD) is presented as a function of pavement age ( $t$ ), as presented in Table 1. Throughout these scenarios, the pavement's age reflects the encountered traffic volumes where the cumulative traffic values are a function of time, the family's expected annual traffic volume, and a fixed growth rate. However, if the pavement experiences varying traffic growth rates, several

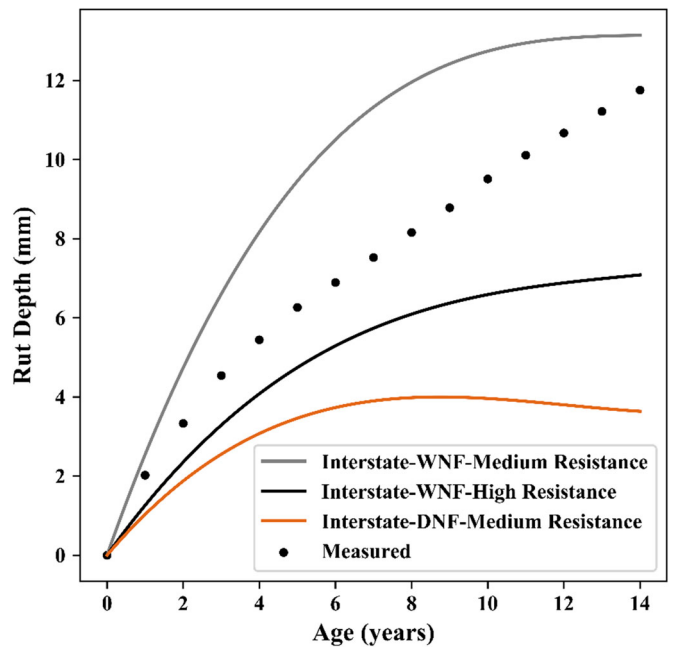


Figure 1. The rutting family curves and measurements used to validate the EnKF framework for LTPP Road 112 Alabama.

adjustments should be incorporated in the framework's implementation, including: (1) monitoring the annual traffic volumes and including these values alongside the rutting depth in the measurement vector ( $d$ ), and (2) incorporating an additional forward propagation model that relates age to annual traffic and updating that when new traffic measurements are obtained.

### 3.3. EnKF mathematical formulation

#### 3.3.1. Sequential data assimilation

Sequential data assimilation (filtering) techniques are applied in situations where the forward propagation of a system's state in time is required. The main goal of this technique is to rectify an initial state estimate using newly collected measurements in order to forecast future states based on the inferred information (Bertino *et al.* 2003). This technique has been previously used in damage detection and online health monitoring of systems (Slika and Saad 2016; Bichara *et al.* 2019).

One of the most widely adopted sequential data assimilation approaches is Kalman filtering (Di Lorenzo *et al.* 2008). The traditional Kalman Filter (KF) approach provides an optimal solution for linear systems subject to additive Gaussian white noise perturbations which restricts its applicability to limited problems (Evensen 2003). Variants of the traditional KF, such as the extended Kalman filter, were developed to

Table 1. Different starting points for EnKF framework.

Scenario	Description	Family			Mathematical Structure: $RD = c_0 + c_1t + c_2t^2 + c_3t^3$
		Traffic	Climate Zone	Resistance	
No. 1	Base Case	Interstate	Wet Non-Freeze	High	$1.10 + 1.35t - 0.091t^2 + 0.0022t^3$
No. 2	Incorrect Mix Performance Family		Wet Non-Freeze	Medium	$1.12 + 2.73t - 0.189t^2 + 0.0044t^3$
No. 3	Incorrect Climate Zone and Mix Performance Family		Dry Non-Freeze	Medium	$2.06 + 1.13t - 0.101t^2 + 0.0028t^3$

perform sequential data assimilation in a broader range of complex and non-linear dynamical systems (Evensen 2002). However, the extended Kalman filter suffers from several shortcomings due to its high computational requirements, bias, and possible divergence potential when estimating highly nonlinear systems or in the presence of non-Gaussian noise (Pham 2001; Evensen 2002). The Ensemble Kalman filter (EnKF) overcomes the previous limitations and outperforms other adaptations of the traditional KF (Pham 2001). EnKF algorithms are attractive due to their applicability to complex non-linear models, non-Gaussian noise, simplicity, and low computational cost (Pham 2001).

In this study, the EnKF is used to develop an updating framework that calibrates the parameters of pavement rutting models. The EnKF algorithm provides a sub-optimal Monte Carlo estimation of the error statistics to propagate an ensemble of model states forward in time. The EnKF algorithm encompasses two steps; the first consists of the prediction or forecasting step, and the second is the update or analysis step. The prediction step entails propagating an ensemble of realizations forward in time based on the current state; then, in the analysis step, the state vectors are updated to minimise the mismatch between the model predictions and actual collected measurements. The EnKF algorithm is presented herein (Evensen 2003; Gillijns *et al.* 2006).

### 3.3.2. Application of EnKF to the rutting model

The same EnKF formulation applies to the three empirical models used to simulate rutting depth. The first step of the EnKF implementation involves evaluating the initial ensemble of state vectors which is created by adding perturbations to a best-guess estimate state vector in a way that properly represents the statistical distributions of the prevailing errors (refer to section 3.4.1 for a discussion about initial errors). In this application, the stochastic state vector  $U$  consists of the progressed rutting depth value (dynamic state variable) as well as the model parameters, as shown in Equation (1).

$$U_t = [\text{RD} \ C_1 \ C_2 \ C_3]^T \quad (1)$$

where  $U_t$  is a realisation of the model state vector at time  $t$ , RD reflects the rutting depth state at time  $t$ , and the  $C_i$ 's represent the rutting propagation model parameters.

At the initialisation stage, which corresponds to a newly constructed pavement, rutting depth ( $\text{RD}_0$ ) is expected to be zero. The model coefficients ( $C_i$ ) are derived from the family models provided in (Haddad *et al.* 2021).

The initial state vector is used to obtain the initial ensemble matrix which reflects the statistical distribution of the initial guess. The initial ensemble matrix is obtained by perturbing the initial state vector by an error value. The ensemble matrix is denoted by  $U$ , as presented in Equation (2).

$$U = (U_1, U_2, \dots, U_N) \in \mathbb{R}^{n \times N} \quad (2)$$

where  $U_i$  is the  $i$ th ensemble member obtained by adding perturbations to the best-guess estimate,  $N$  is the number of ensemble members determined through sensitivity analysis, and  $n$  is the size of the model state vector.

The ensemble mean ( $\bar{U}$ ) is then evaluated using Equation (3).

$$\bar{U} = U1_N \in \mathbb{R}^{n \times N} \quad (3)$$

where  $1_N \in \mathbb{R}^{N \times N}$  is a matrix having its elements equal to  $1/N$ .

The ensemble covariance matrix  $P_e$  is computed using Equation (4).

$$P_e = \frac{(U - \bar{U})(U - \bar{U})^T}{N - 1} \in \mathbb{R}^{n \times n} \quad (4)$$

In the forecast or prediction step, the forward model is used to propagate rutting from timestep  $(t - 1)$  to timestep  $(t)$ , as presented in Equation (5).

$$U_{t,i}^f = f(U_{t-1,i}^a) + \varepsilon_i \quad i \in [1, N] \quad (5)$$

where  $U_{t,i}^f$  is the forecasted state vector at time  $(t)$  corresponding to the  $i$ th ensemble,  $f(\dots)$  is the mathematical representation of the rutting forward propagation model,  $U_{t-1,i}^a$  is the updated state vector at time  $(t - 1)$  corresponding to the  $i$ th ensemble, and  $\varepsilon_i$  is the process noise having a zero mean and a covariance representing the model error.

Here, realizations of the rut depth (RD) of the state vector are propagated forward in time using the governing dynamical equations. The dynamic model is represented by an ordinary differential equation (ODE) which reflects the incremental variation of rut depth as a function of time, as presented in Equation (6). Equation (6) represents this study's implementation of the ' $f(\dots)$ ' component presented previously in Equation (5). It is worth noting that pavement age is the only factor considered in the model since the utilised dataset did not have temporal measurements of other factors (such as traffic) to perform the updates accordingly.

$$\frac{d(\text{RD})}{dt} = c_1 t^0 + 2c_2 t^1 + 3c_3 t^2 = C_1 + C_2 t + C_3 t^2 \quad (6)$$

This derivation is demonstrated for scenario No. 1 in Equation (7).

$$\begin{aligned} & \frac{d(1.10 + 1.35t - 0.091t^2 + 0.0022t^3)}{dt} \\ & = 1.35 - 0.182t + 0.0066t^2 \end{aligned} \quad (7)$$

The dynamic rutting model parameters ( $C_i$ ), that are derived from Equation (6), are incorporated in the initial state vector which holds the parameters and dynamic variables that the EnKF framework intends to monitor and update. The initial state vectors for each of the three scenarios are provided in Table 2.

The Forward Euler Discretization time integration method is implemented to propagate the system state forward in time at a 0.01-year time-step for all the ensemble members. The mathematical representation of the rutting propagation model incorporated in the EnKF is presented in Equation (8).

$$\text{RD}_{t+1} = \left( \text{RD}_t + \Delta t \times \frac{d(\text{RD})}{dt} \right) + \epsilon \quad (8)$$

where  $\text{RD}_t$  is the predicted rut depth at time  $t$ ,  $\Delta t$  is the model progression time-step that is equivalent to 0.01 years, and  $\epsilon$

**Table 2.** Initial guess for the state vectors corresponding to each scenario

Scenario	$RD_0$	Parameter 1 ( $C_1$ )	Parameter 2 ( $C_2$ )	Parameter 3 ( $C_3$ )
No. 1	0	1.35	-0.182	0.0066
No. 2	0	2.73	-0.379	0.0132
No. 3	0	1.13	-0.203	0.0084

represents the model error (refer to section 3.4.2 for a discussion of model errors). The forward propagation time-step is determined based on sensitivity analysis to find an appropriate time-step that minimises the approximation error, as demonstrated in Figure 2. For illustrative purposes, this figure indicates the implications of changing the step size on the accumulation of approximation inaccuracies for the predictions corresponding to scenario No. 1. The figure shows that the accumulated approximation errors increase as a function of the time-step.

In the analysis or update step, the forecasted ensemble of state vectors ( $U_t^f$ ) is updated based on a vector of measurements ( $d$ ).  $N$  vectors of the perturbed observations are obtained after incorporating the error ( $\varepsilon_j$ ) associated with the measurement uncertainty, as shown in Equation (9). The measurement vectors ( $d_j$ ) are then stored in an ensemble of observations ( $D$ ), as presented in Equation (10) where  $m$  is the number of collected data points at a given time:

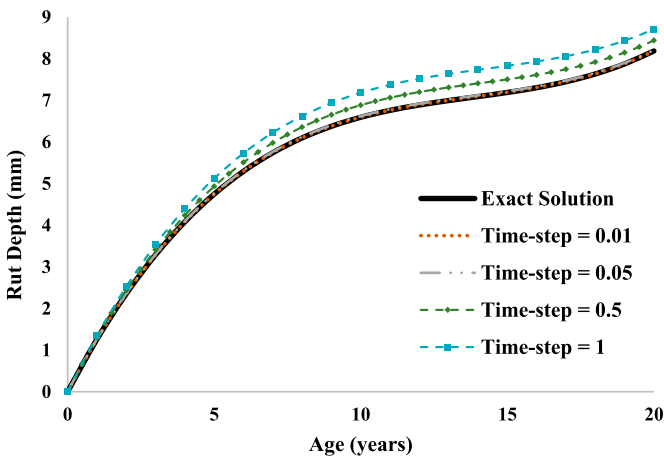
$$d_j = d + \varepsilon_j \quad j \in [1, N] \quad (9)$$

$$D = (d_1, d_2, \dots, d_N) \in R^{m \times N} \quad (10)$$

In this application, field rutting measurements are sequentially used to calibrate the model parameters. The update frequency reflects typical distress survey timings, which are typically conducted on an annual basis. Each year, rutting observations are collected and used to update the model while taking the associated uncertainties into account (refer to section 3.4.4 for a discussion of measurement errors).

The corresponding measurement error covariance matrix  $R_e$  is defined in Equation (11).

$$R_e = \frac{\gamma\gamma^T}{N-1} \in R^{m \times m} \quad (11)$$

**Figure 2.** Forward Euler rutting approximation results as a function of the time-step size.

where  $\gamma = (\varepsilon_1, \varepsilon_2, \dots, \varepsilon_N) \in R^{m \times N}$  is the ensemble of measurement perturbations.

The updated ensemble of states at time step ( $t$ ) is then computed through Equation (12).

$$U_t^a = U_t^f + K_t(D_t - HU_t^f) \quad (12)$$

where  $K_t$  is the Kalman Gain which is formulated in Equation (13),  $H \in R^{m \times n}$  is the observation matrix that relates the ensemble of state vectors to the measured variables.

$$K_t = P_e H^T (H P_e H^T + R_e)^{-1} \quad (13)$$

The updated ensemble of the model parameters is finally used to estimate and predict the dynamic states of the system with enhanced accuracy.

### 3.4. Uncertainty quantification

Several sources of uncertainty should be considered and quantified in prognostic formulations of naturally occurring phenomena. These uncertainties can be attributed to the adopted mathematical models and measurement processes. The quantification of the different sources of uncertainty is discussed herein and the results are summarised in Table 3.

#### 3.4.1. Initial guess error

Uncertainty in the initial guess of the model states reflects the confidence in the selected model parameters to represent existing conditions. This error is expected to be higher when sufficient information to select an appropriate family curve is not available. For practicality purposes, this error is represented as an additive Gaussian noise with a coefficient of variation (C.O.V.) of 20% for all scenarios.

#### 3.4.2. Model error

Mathematical and empirical models cannot simulate natural phenomena with absolute accuracy. Model errors arise from simplifications or imperfections associated with the adopted mathematical structure or unknown details that cannot be identified and incorporated. In this implementation, the model error is quantified for each family model independently using rutting depth measurements obtained from the LTPP. Figure 3 shows an example of the measured rutting values as well as the predictions corresponding to the generic curve of scenario No.1. The mismatch between the measurements (cross marker) and predictions (solid line) stems from the existing model error that is estimated by averaging the individual percentage errors for each measurement data point. Figure 3 also presents data labels for a selection of individual percentage errors reflecting the percentage difference between the simulated and measured data at different instants. The model error is similarly quantified for the two other scenarios proposed in Table 1 and represented as an additive Gaussian white noise with a C.O.V. equivalent to the average residual errors of the data points.

#### 3.4.3. Parametric error/process noise

Parametric uncertainty arises from limitations in the amount of data available to estimate the parameters. The parametric

**Table 3.** Quantified uncertainty in the EnKF framework.

Source of Uncertainty		Distribution	Standard Deviation	Quantification Method
Initial Estimate Error		Normal	20% of mean value	Sensitivity analysis
Model Error		Normal	Scenario No. 1: 20% Scenario No. 2: 10% Scenario No. 3: 18%	Family curves residuals
Process Noise		Normal	1% of mean value	Sensitivity analysis
Measurement Error	Instrumentation	Uniform	$\pm 2$ mm of mean value	Literature review
	Spatial Variability	Normal	20% of mean value	Variability in LTPP data

error or process noise is represented as an additive Gaussian noise with a C.O.V. of 1% obtained from sensitivity analysis.

### 3.4.4. Measurement error

The sources of error associated with rut depth measurements are twofold. The first source of measurement error is associated with the accuracy and reliability of the used instruments. The second source of uncertainty consists of the spatial variability caused by imperfections in the pavement construction and compaction processes, as well as the randomness of the lateral position of the vehicles' tire loads on the pavement, known as wheel wander. In practice, this type of variability is observed when measuring the rutting depth at different locations within the same road or same pavement family and quantified as the standard deviation between these measurement values. Based on the literature, instrumentation errors are estimated at 2 mm (Jeyapalan *et al.* 1987; Simpson 1999; National Academies of Sciences, Engineering, and Medicine 2004; Pierce *et al.* 2013; Wang *et al.* 2017). Therefore, the instrumentation error is represented by a Uniform distribution bound between  $-2$  and  $2$ . In addition, an additive Gaussian white noise perturbation with a C.O.V. obtained from the variability in the available data is used to simulate the spatial variability. While a C.O.V of 20% is used in this study, a road agency can evaluate its observed spatial variability based on engineering judgment or available rutting measurements.

## 4. Results and analysis

The EnKF framework utilises a set of measurement data to update an initial guess corresponding to the parameters of rutting generic curves. Following each update step, the newly obtained model parameters are employed to forecast the rut depth at future years. To assess the robustness and applicability of the framework, sensitivity analysis is conducted by varying several contributing factors such as the effect of the ensemble size, initial guesses, and frequency of updates.

### 4.1. Sensitivity to the ensemble size

The sensitivity of the EnKF framework to the ensemble size is evaluated to obtain the optimal number of ensembles that provides the required accuracy and guarantees the consistency of the results. To that extent, the simulation is performed 100 times for each ensemble size being investigated to calculate the mean and standard deviation of the predicted parameters following the final update step.

Figure 4 presents the results of the sensitivity analysis corresponding to the third parameter ( $C_3$ ) and shows the variability of the mean and standard deviation of the updated parameters across the different simulations. The variability between the means of the predicted parameters of the different simulation runs decreases as the ensemble size increases. The variability achieved at an ensemble size of 10,000 is considered

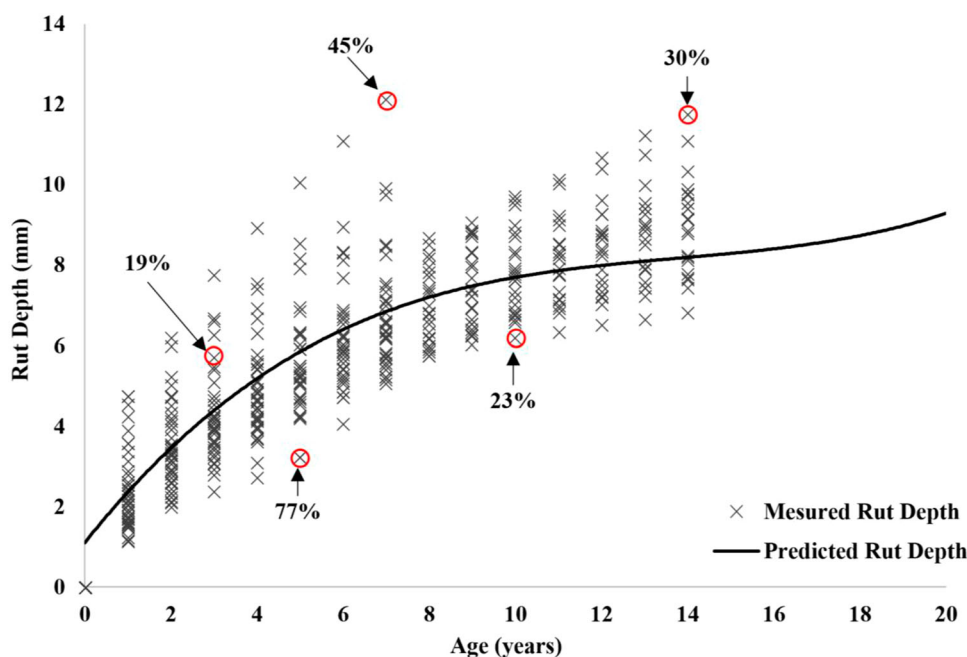


**Figure 3.** Error quantification for the predictive model used for simulating rutting depth for the interstate, wet non-freeze, and good performance pavement family. Percentages depict percentage error in prediction

acceptable and it will be used for all the subsequent simulations in this study. A higher number of ensembles would drastically increase the computational requirements without having significant benefits to the accuracy and repeatability of the results. While Figure 4 only shows the sensitivity analysis results of  $C_3$  for demonstrative purposes, the observations are in fact representative of all other parameters.

#### 4.2. Sensitivity to the initial guess

Sensitivity analysis is also conducted to evaluate the robustness of the framework and its ability to converge despite the selected initial states. The framework is assessed using initial state vectors corresponding to three different family curves as presented previously in Table 1.

The EnKF framework is run for each of the three cases to obtain the probabilistic characteristics of the model parameters following every update step. A Monte Carlo simulation with 1000 realizations of the updated parameters is carried out to evaluate the distribution of the predicted rutting depths at different stages. Figures 5a, 6a, and 7a depict the mean forecasted rutting depths starting from age zero and using the updated model parameters for each initial estimate scenario. An envelope representing one standard deviation away from the prediction mean of the final update is also shown. Additionally, the mean discrepancy between the predicted and measured rutting values following each update step is computed to assess and compare the performance of the three rutting propagation models, as provided in Equation (14). Figures 5b, 6b, and 7b show the evolution of the average prediction error as a function of the number of EnKF updates calculated as:

$$\text{Mean Percentage Error (\%)} = \frac{100}{N} \times \sum_{i=1}^N \frac{|RD_{\text{measured}}^i - RD_{\text{predicted}}^i|}{RD_{\text{measured}}^i} \quad (14)$$

where  $N$  is the number of Monte Carlo simulations (i.e. 1,000),  $RD_{\text{predicted}}^i$  is the predicted rut depth at point  $i$ ,  $RD_{\text{measured}}^i$  is the measured rut depth corresponding to the predicted value at  $i$ .

Figure 5a shows that the initial model parameters corresponding to the base case scenario significantly underestimate the extent of rutting. The accuracy of the forecasted rutting depth improved significantly after the first update at year 1. Additional improvements are achieved after updating the model parameters a second time using the set of measurements obtained at year 2. As more rutting data points become available, the incremental improvement in the forecasted state becomes less significant, as shown in Figure 5a. The substantial improvement in the prediction accuracy after the first two updates signifies the efficacy of the EnKF updating framework even with a limited amount of measurement data.

Moreover, Figure 5b presents the average of the errors computed for all 1,000 simulations following each update. The figure reveals a sharp drop (58%) in the average percentage error from 30% corresponding to the initial prediction to 12.4% after the second update. Beyond that, the prediction errors are further improved by a total of 8% to reach an average prediction error of approximately 10% after the final update where all the available measurements are used for model calibration.

Figure 6a shows that the model parameters based on Scenario No. 2 in Table 1, which corresponds to an incorrect rutting resistance level and consequently over-predict rutting. We notice that after observing the first measurement at year 1, the Kalman filter realises that the initial prediction was significantly over-predicting rutting and produces the updated grey curve which exhibits lower rutting predictions. Although a significant improvement in the average percentage error is obtained after the first update, the updated model at year 1 fails to accurately predict rutting depth beyond year 8, after which the forecasted rutting exhibits an unrealistic decreasing trend. This decreasing trend in the updated rutting models persists until the fifth update (black curve). After observing more than five years of rutting measurements, the Kalman filter becomes able to reconcile the differences between the initial incorrect generic model and the actual rutting behaviour. Specifically, more accurate representations of the propagation of rutting are obtained after the tenth and fourteenth updates. This is also depicted in Figure 6b where the average percentage prediction error decreases to approximately 15% after the final update. Consequently, we conclude that the

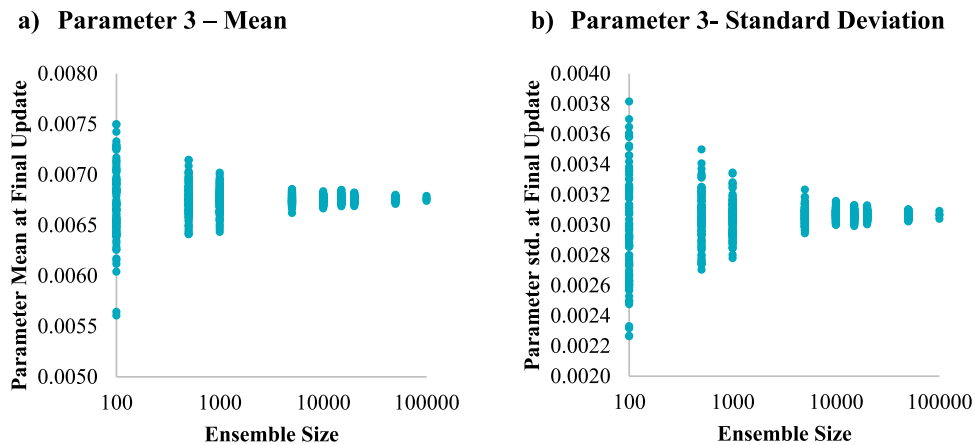


Figure 4. Mean and standard deviation of the updated values of parameter 3 as a function of the ensemble size.

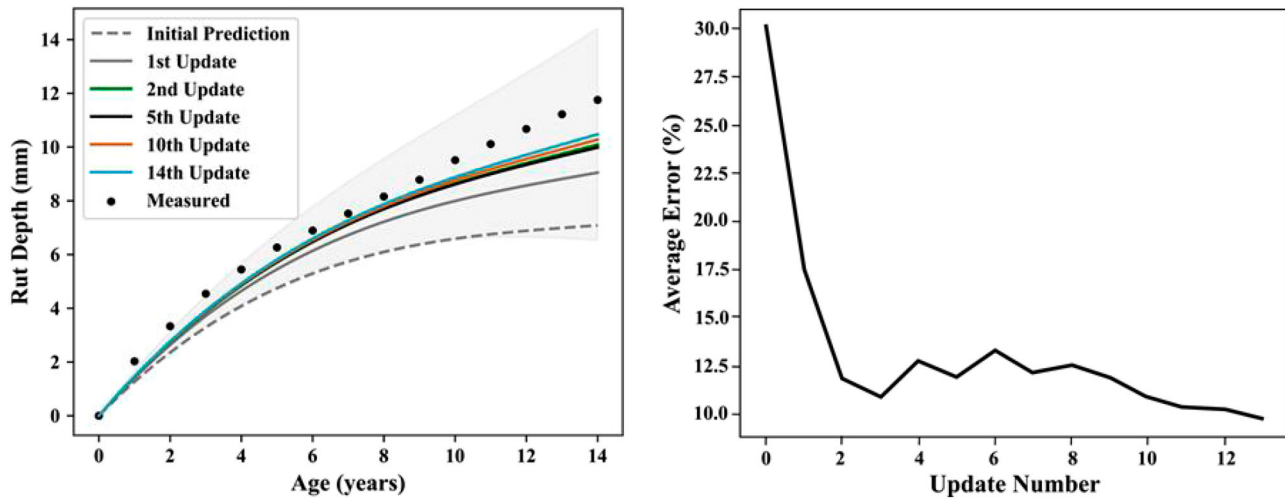


Figure 5. Base case model results: (a) rut depth predictions and (b) model performance as a function of the number of EnKF updates.

updating procedure is sensitive to the mix performance where more measurements are required to achieve a realistic and reliable model.

Similarly, Figure 7a shows the evolution of the rutting forecast based on the EnKF updates for Scenario No. 3 in Table 1 representing an incorrect rutting performance level and climate zone family. The figure shows that the initial prediction significantly underpredicts rutting while a 50% improvement in the average percentage errors occurs after the first two updates. The initial underprediction is expected because the generic curve corresponds to a DNF climate zone which experiences less rutting than WFN zones. As more rutting measurements become available to update the model's parameters, further improvements are observed and the average error in the rutting prediction at the final update reaches 20%, as shown in Figure 7b.

Although the accuracy of the EnKF estimates varies among the three scenarios, the measurements remain almost within one standard deviation from the predicted mean, as depicted by the grey envelope in Figures 5a, 6a, and 7a. Additionally, as evident from the results of Figures 5b, 6b, and 7b, the improvements in the average predictive performance of the

three scenarios are consistent and comparable, and the framework reduces the prediction percentage errors by an average of 60% between the initial state and the final update. Therefore, the presented scheme is robust and capable to converge to the true state even if the initial estimate is highly inaccurate.

The convergence of the state vector is also illustrated in Figure 8 for each of the initial estimate scenarios. Figure 8 presents comparisons between the real-time updated mean of the rutting depth obtained using the EnKF scheme with one-year update frequency, the initial prediction, and the measured data. The figures also show an envelope representing a range of one standard deviation away from the mean predicted rutting depths. The graphs in Figure 8 indicate how the EnKF framework succeeds in improving the predictions after every update step; thus, confirming the convergence of rutting predictions to the true state.

#### 4.3. Sensitivity to the update frequency

Sensitivity analysis is performed to study the effect of the update frequency on the robustness of the proposed

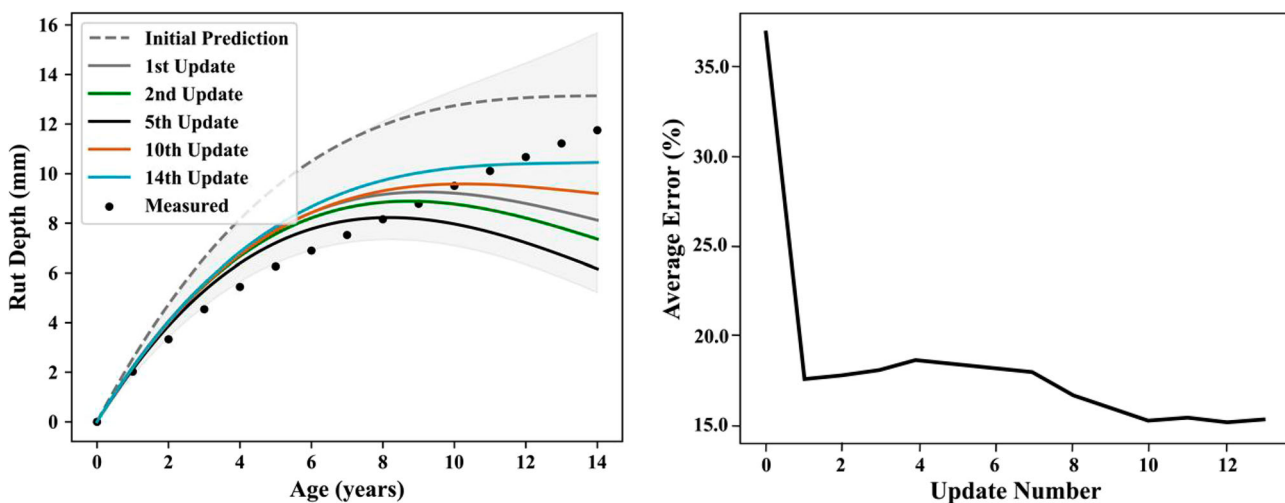


Figure 6. Incorrect rutting resistance case model results: (a) rut depth predictions and (b) model performance as a function of the number of EnKF updates.

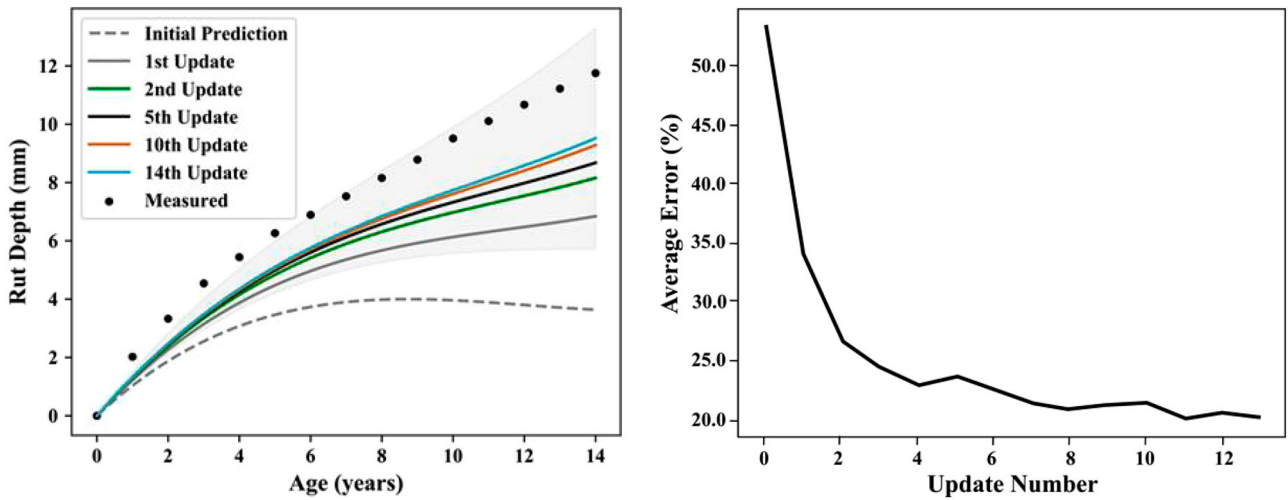


Figure 7. Incorrect Climate Zone and Rutting Resistance case model results: (a) rut depth predictions and (b) model performance as a function of the number of EnKF updates.

framework and its capability to converge to the true state. This analysis was only applied to Scenario No. 1 for illustrative purposes. While a one-year update frequency was adopted in

previous analyses to reflect common distress survey schedules, studying the effect of the update frequency has significant implications on policy. Identifying the lowest possible update

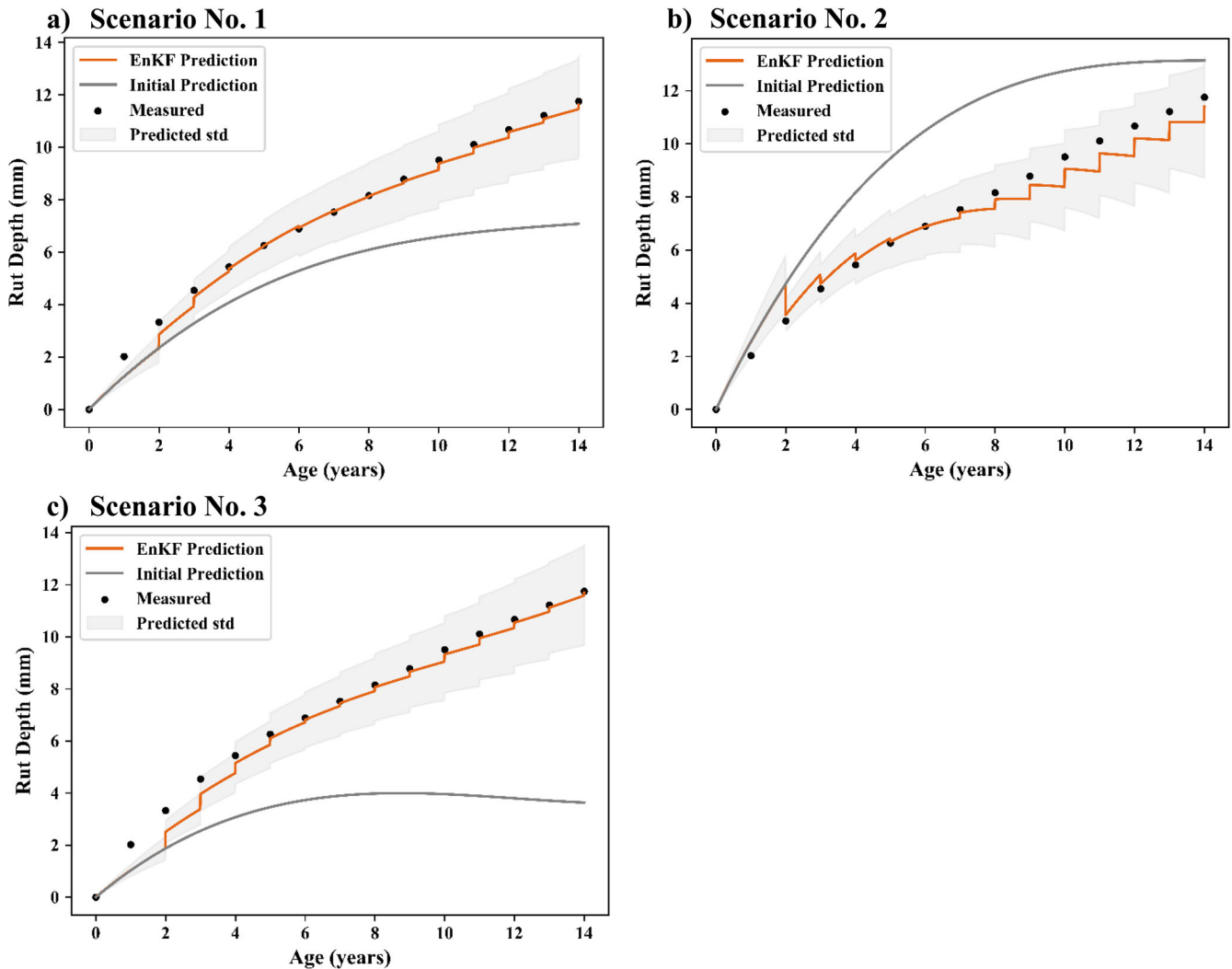


Figure 8. Real-time updated vs. measured rutting depth following each EnKF update for: (a) Scenario No. 1, (b) Scenario No. 2, and (3) Scenario No. 3.

frequency that guarantees convergence allows road agencies to relax their rutting measurement intervals and leads to significant savings without sacrificing predictive accuracy. Table 4 presents the residual errors corresponding to the outcome of the update schemes corresponding to 1, 2, 3, and 4-year update frequencies. Moreover, Table 4 indicates the obtained average percentage of errors at ages 6, 9, and 12 years. Figure 9 presents the real-time updated mean rutting prediction corresponding to the examined update frequencies. The figure shows that the 1 and 2-year update intervals converge faster to the true state compared to the larger intervals. The results depicted in Figure 9 and Table 4 confirm that the average residual errors increase as a function of the update frequency, which is in line with original expectations. Therefore, a 1 or 2-year update interval guarantees an optimal solution, while road agencies may opt for a 3-year interval that is associated with a slightly higher error.

#### 4.4. Discussions

This section presents a more detailed discussion of the results and the practical and policy implications of the proposed framework. For illustration purposes, this section focuses on evaluating the base case scenario (i.e. Scenario No.1 in Table 1). As mentioned previously, the probabilistic characteristics of the 10,000 ensembles of the updated model parameters are determined after every measurement. The Chi-Squared test is then applied to identify the ideal probability distribution for each updated parameter. Although the parameters were initially considered independent and normally distributed at the initial stage of the EnKF framework, the calibrated states possessed different characteristics. A correlation of  $-0.2$  exists between parameters 1 and 2 and  $-0.1$  between parameters 2 and 3. Table 5 shows the corresponding distribution and covariance of the parameters after the final update. The determined distribution and covariance of the calibrated parameters are utilised to sample realizations through Monte Carlo simulations. One thousand realizations of the three parameters, as introduced in section 4.2, are sampled to study the variability in the predicted rutting depth.

Figure 10 shows the mean and standard deviation of the predictions after the final update as well as the measurements and their associated uncertainty. The figure emphasises the relatively large variability in rutting measurements and demonstrated how the updated model accounts for it. Therefore, the results show that the proposed framework achieves its objectives as it reduces the mismatch between the measurements and the predictions. Additionally, it allows for modelling the uncertainties and

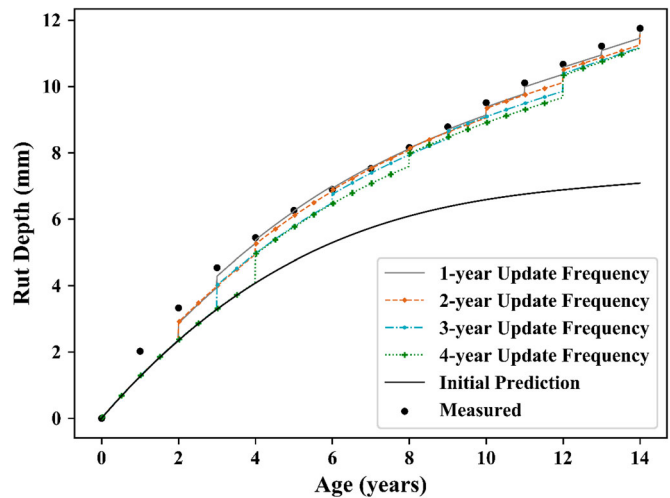


Figure 9. Real-time updated rutting depth as a function of update frequency.

overcoming the limitations associated with deterministic models. Although the prediction interval which delineates where future observations may fall is relatively wide, the results are considered acceptable provided the high uncertainties associated with measuring and predicting rutting in asphalt pavements.

From practice and policy perspectives, the power of the proposed methodology lies in its ability to provide accurate predictions that practitioners can employ in pavement management. In this application, rut depths exceeding 6 mm are set as triggers for milling and overlaying, while pavements exhibiting rutting depths beyond 13 mm are candidates for rehabilitation by removing the distressed area, as suggested in AASHTO's Guide Specifications for Highway Construction (AASHTO 2008). Given that treating the pavement is required when the rut depth exceeds 6 mm, maintenance will be planned at year 8 if the initial model parameters were used to predict rutting, while it will be planned 3 years earlier if the updated model, which overlaps with the measurements, was used instead (Figure 10). As such, the proposed framework ensures a more efficient and effective maintenance management system.

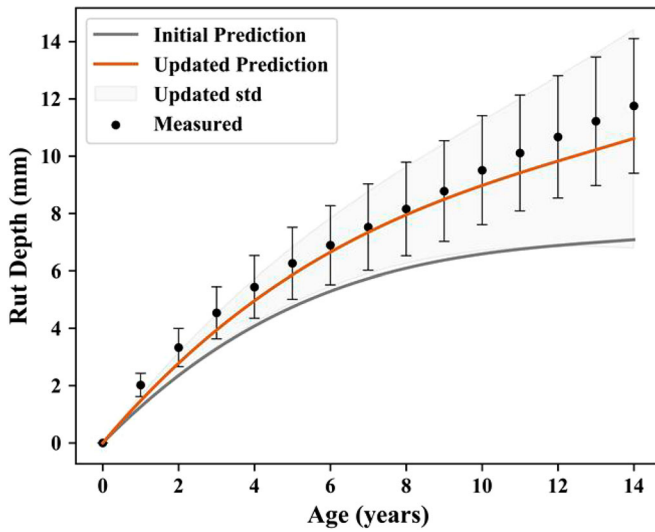
In addition to obtaining a prediction curve, the framework can be used to develop maintenance schedules by providing engineers with the probability of reaching specific maintenance thresholds. This probability is computed by evaluating the percentage of the predicted rutting depth values, which were obtained from the Monte Carlo simulations, that range between 6 and 13 mm or exceed 13 mm at each pavement

Table 4. Average error for rutting prediction for different update frequencies.

Update Frequency (years)	Average Rutting Prediction Error (%)		
	Year-6	Year-9	Year-12
1	12.7	11.3	10.1
2	11.7	11.2	10.6
3	12.8	11.8	11.6
4	16.9	14.0	12.3

Table 5. Calibrated model parameters distribution after the final update for the base case scenario.

Parameters	Distribution	Mean	Covariance matrix		
Parameter 1	Lognormal	1.54	1.03 e-05	-1.56 e-03	4.02 e-02
Parameter 2	Beta	-0.176	-3.94 e-06	1.10 e-03	-1.56 e-03
Parameter 3	Lognormal	0.00667	1.82 e-06	-3.94 e-06	-1.03 e-05



**Figure 10.** The calibrated rutting prediction model compared to field rutting and measurement uncertainty presented by the error bars.

age (Equation (15) and (16)).

$$\text{Probability Maintenance}_n = \frac{\text{CountIf}(6 \text{ mm} < \text{RD}_{\text{predicted}}^n < 13 \text{ mm})}{N} \quad (15)$$

$$\text{Probability Rehabilitation}_n = \frac{\text{CountIf}(\text{RD}_{\text{predicted}}^n > 13 \text{ mm})}{N} \quad (16)$$

where  $n$  is the age of the pavement associated with the probability being calculated, CountIf is a function that counts the number of occurrences satisfying predefined conditions,  $N$  represents the 1,000 Monte Carlo simulations, and  $\text{RD}_{\text{predicted}}^n$  corresponds to all the simulated rutting depths at age  $n$ .

This is demonstrated in Figure 11 which shows the probability of requiring milling and resurfacing or rehabilitation each year. This concept can be interpreted on the project and network levels. On the project level, the outcome provides engineers with the probability that a road may require a certain treatment type. On the network level, the outcome is interpreted as the percentage of the entire network requiring each treatment type. For instance, 80% of the roads corresponding to this pavement family will require milling in the 8th year of the pavement's life. Beyond the 8 years mark, the percentage of pavements that need rehabilitation rises while that requiring milling and resurfacing decreases.

## 5. Conclusions

This research study is motivated by the rapidly increasing global pavement monitoring and management efforts. Such efforts provide local road agencies that generally rely on generic and knowledge-based pavement performance prediction models with the opportunity to continuously improve and calibrate their models, ultimately, enhancing the efficiency of their pavement management practices and the sustainability of their pavement infrastructure.

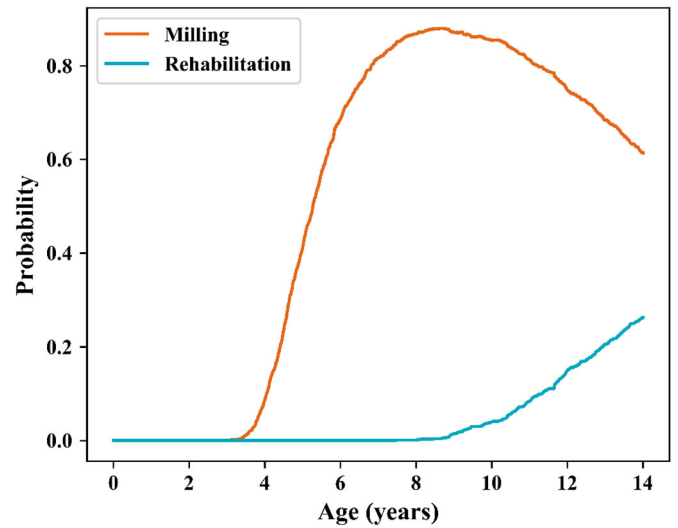


**Figure 11.** Probability of reaching maintenance triggers.

This study presents a novel stochastic framework based on the implementation of the EnKF algorithm to accurately predict rutting in asphalt pavements. This framework which aims at updating and calibrating model parameters was validated using a set of generic family curves and a set of rutting measurements extracted from the LTPP. The main conclusions of the presented analyses and results are summarised as follows:

- A sensitivity analysis performed on the ensemble size reveals that a relatively large ensemble size of 10,000 is needed to attain sufficiently high precision in estimating the parameters due to the high levels of uncertainty present.
- The results are consistent among the three examined initial state estimates and reveal that the accuracy of the predictions remains within tolerable limits when the initial states are varied.
- The presented framework calibrates the governing parameters of the rutting prediction models and reduces the mismatch between the measurements and predictions by up to 60% on average.
- The examined numerical application confirms that the EnKF framework is capable of assisting engineers in monitoring pavement rutting and determining the probability of requiring maintenance. Consequently, it succeeds in enhancing the efficiency of the adopted pavement management systems.

A shortcoming of the research presented in this paper is that it does not consider cases where the traffic growth rate varies with time. The dataset used in this study did not have the information required for modelling such scenarios.

In conclusion, this study paves the way for further research to integrate a similar framework with different types of pavement performance models. This approach will lead to developing comprehensive and adaptive pavement management systems that incorporate online model calibration whenever new measurements are collected.

## Disclosure statement

No potential conflict of interest was reported by the authors.

## ORCID

Angela J. Haddad  <http://orcid.org/0000-0001-5759-2260>

George A. Saad  <http://orcid.org/0000-0002-5938-6265>

Ghassan R. Chehab  <http://orcid.org/0000-0001-5779-3046>

## References

- AASHTO, 2008. *Guide specifications for highway construction*. 9th ed. American Association of State Highway and Transportation Officials (AASHTO). <https://books.google.com.lb/books?id=E4MzYL7S0AMC>.
- AASHTO, 2012. *Pavement management guide*. 2nd ed. Washington, DC: American Association of State Highway and Transportation Officials.
- AASHTO, 2015. *Mechanistic-empirical pavement design guide: a manual of practice*. Washington, DC: American Association of State Highway and Transportation Officials. <https://books.google.co.il/books?id=dduLtAEACAAJ>.
- Abambres, M., and Ferreira, A., 2018. Application of ANN in pavement engineering: state-of-art. *ViXra*. doi:10.31224/osf.io/nh8k6.
- Abaza, K.A., 2016. Simplified staged-homogenous Markov model for flexible pavement performance prediction. *Road Materials and Pavement Design*, 17, 365–381.
- Abu-Ennab, L.B., 2015. *Developing pavement performance prediction models for the state of Arkansas*. Little Rock, Arkansas: University of Arkansas at Little Rock.
- Amador-Jiménez, L., and Mrawira, D., 2012. Bayesian regression in pavement deterioration modeling: revisiting the AASHO road test Rut depth model. *Infrastructura Vial*, 14, 28–35.
- ASCE, 2017. *2017 infrastructure report card*. Reston, VA: ASCE.
- ASTM, ASTM D6433-20, 2020. Standard practice for roads and parking lots pavement condition index surveys. doi:10.1520/D6433-20.
- Baladi, G.Y., et al., 2017. *Pavement performance measures and forecasting and the effects of maintenance and rehabilitation strategy on treatment effectiveness*. Maclean, Virginia: Federal Highway Administration.
- Bannour, A., et al., 2019. Optimization of the maintenance strategies of roads in Morocco: calibration study of the degradations models of the highway development and management (HDM-4) for flexible pavements. *International Journal of Pavement Engineering*, 20, 245–254.
- Bertino, L., Evensen, G., and Wackernagel, H., 2003. Sequential data assimilation techniques in oceanography. *International Statistical Review*, 71, 223–241.
- Bichara, L., Saad, G., and Slika, W., 2019. Probabilistic identification of the effects of corrosion propagation on reinforced concrete structures via deflection and crack width measurements. *Materials and Structures*, 52, 89. doi:10.1617/s11527-019-1389-y.
- Choi, S., and Do, M., 2020. Development of the road pavement deterioration model based on the deep learning method. *Electronics*, 9. doi:10.3390/electronics9010003.
- Choummavong, L., and Martin, T., 2010. Interim network level functional road deterioration models, Austroads Publ. No. AP-T158/10, ARRB.
- Di Lorenzo, E., et al., 2008. Theory and applications of variational, sequential and Bayesian hierarchical methods in data assimilation. *AGU Fall Meeting Abstract*.
- Ekblad, J., et al., 2021. Impact on rutting from introduction of increased axle loads in Finland. *International Journal of Pavement Engineering*, 1731–1743. doi:10.1080/10298436.2020.1721497.
- Elkins, G.E., et al., 2018. *Long-term pavement performance information management system user guide*. McLean, VA. <https://trid.trb.org/view.aspx?id=697916>
- Evensen, G., 2002. *Sequential data assimilation for nonlinear dynamics: the ensemble Kalman filter*, *Ocean forecast*. Berlin, Heidelberg: Springer, 97–116.
- Evensen, G., 2003. The ensemble Kalman filter: theoretical formulation and practical implementation. *Ocean Dynamics*, 53, 343–367. doi:10.1007/s10236-003-0036-9.
- FHWA, 2018. *Transportation asset management plan development processes certification and recertification guidance*. Washington, DC. Available from: <https://www.fhwa.dot.gov/asset/guidance/certification.pdf> (Accessed 20 Feb 2020).
- Fwa, F.T., Pasindu, H. R., and Ong, G. P., 2012. Critical rut depth for pavement maintenance based on vehicle skidding and hydroplaning consideration. *Journal of Transportation Engineering*, 138, 423–429. doi:10.1061/(ASCE)TE.1943-5436.0000336.
- George, K.P., 2000. *MDOT pavement management system: prediction models and feedback system*. Mississippi: Dept. of Transportation.
- Gillijns, S., et al., 2006. What is the ensemble Kalman filter and how well does it work? In: *2006 American Control Conf., IEEE*, 6.
- Gong, H., et al., 2018. Improving accuracy of rutting prediction for mechanistic-empirical pavement design guide with deep neural networks. *Construction and Building Materials*, 190, 710–718.
- Gonzalo, R., et al., 2018. Network-level pavement structural evaluation. *Journal of Infrastructure Systems*, 24, 04018033. doi:10.1061/(ASCE)IS.1943-555X.0000454.
- Haddad, A.J., Chehab, G.R., and Saad, G.A., 2021. The use of deep neural networks for developing generic pavement rutting predictive models. *International Journal of Pavement Engineering*, 1–17. doi:10.1080/10298436.2021.1942466.
- Hjelle, H.M., 2007. A model for estimating road wear on in-service roads. *International Journal of Pavement Engineering*, 8, 237–244. doi:10.1080/10298430600677453.
- Hong, F., and Prozzi, J.A., 2006. Estimation of pavement performance deterioration using Bayesian approach. *Journal of Infrastructure Systems*, 12, 77–86.
- Inkoom, S., et al., 2020. Assessment of deterioration of highway pavement using Bayesian survival model. *Transportation Research Record: Journal of the Transportation Research Board*, 2674, 310–325. doi:10.1177/0361198120919112.
- Jain, S.S., Parida, M., and Thube, D.T., 2007. HDM-4 based optimal maintenance strategies for low-volume roads in India. *Road & Transport Research*, 16, 3.
- Jeyapalan, K., Cable, J.K., and Welper, R., 1987. Iowa DOT evaluation of the PASCO road survey system.
- Jiménez, L.A., and Mrawira, D., 2012. Bayesian regression in pavement deterioration modeling: revisiting the AASHO road test rut depth model. *Transportation Research Record*, 28–35.
- Khan, M.U., et al., 2014. Developing a new road deterioration model incorporating flooding. *Proceedings of the Institution of Civil Engineers – Transport*, 167 (5), 322–333.
- Li, N., Haas, R., and Xie, W.-C., 1997. Development of a new asphalt pavement performance prediction model. *Canadian Journal of Civil Engineering*, 24, 547–559.
- Li, Q.J., et al., 2019. Data needs and implementation of the pavement ME design. *Transportmetrica A: Transport Science*, 15, 135–164. doi:10.1080/23249935.2018.1504254.
- LTPP InfoPave, n.d. Available from: <https://infopave.fhwa.dot.gov/?Goto=Home> [Accessed 15 Dec 2020].
- Luo, Z., et al., 2016. Bayesian updating approach for flexible pavements considering fatigue and rutting failures. *Journal of Testing and Evaluation*, 44, 20140356–20140533. doi:10.1520/JTE20140356.
- Mamlouk, M., et al., 2018. Effects of the international roughness index and rut depth on crash rates. *Transportation Research Record: Journal of the Transportation Research Board*, 2672, 418–429. doi:10.1177/0361198118781137.
- National Academies of Sciences, Engineering, and Medicine. 2004. *Automated pavement distress collection techniques*. Washington, DC: The National Academies Press.
- Osorio-Lird, A., et al., 2018. Application of Markov chains and Monte Carlo simulations for developing pavement performance models for urban network management. *Structure and Infrastructure Engineering*, 14, 1169–1181. doi:10.1080/15732479.2017.1402064.

- Pais, J.C., Amorim, S. I. R., and Minhoto, M.J.C., 2013. Impact of traffic overload on road pavement performance. *Journal of Transportation Engineering*, 139, 873–879. doi:10.1061/(ASCE)TE.1943-5436.0000571.
- Park, E.S., et al., 2008. A Bayesian approach for improved pavement performance prediction. *Journal of Applied Statistics*, 35, 1219–1238.
- Pérez-Acebo, H., et al., 2018. Research trends in pavement management during the first years of the 21st century: A bibliometric analysis during the 2000–2013 period. *Applied Sciences*, 8, 1041.
- Pham, D.T., 2001. Stochastic methods for sequential data assimilation in strongly nonlinear systems. *Monthly Weather Review*, 129, 1194–1207.
- Pierce, L.M., McGovern, G., and Zimmerman, K.A., 2013. *Practical guide for quality management of pavement condition data collection*. Washington, DC: United States Federal Highway Administration.
- Pulugurta, H., Shao, Q., and Chou, Y.J., 2013. Pavement condition prediction using Markov process. *Journal of Statistics and Management Systems*, 12, 853–871. doi:10.1080/09720510.2009.10701426.
- Saha, P., Ksaibati, K., and Atadero, R., 2017. Developing pavement distress deterioration models for pavement management system using markovian probabilistic process. *Advances in Civil Engineering*, 2017, 1–9. doi:10.1155/2017/8292056.
- Salama, H.K., Chatti, K., and Lyles, R.W., 2006. Effect of heavy multiple axle trucks on flexible pavement damage using In-service pavement performance data. *Journal of Transportation Engineering*, 132, 763–770. doi:10.1061/(ASCE)0733-947X(2006)132:10(763).
- Simpson, A.L., 1999. Characterization of transverse profile. *Transportation Research Record: Journal of the Transportation Research Board*, 1655, 185–191.
- Slika, W., and Saad, G., 2016. An ensemble Kalman filter approach for service life prediction of reinforced concrete structures subject to chloride-induced corrosion. *Construction and Building Materials*, 115, 132–142. doi:10.1016/j.conbuildmat.2016.04.025.
- Tabatabaee, N., and Ziyadi, M., 2013. Bayesian approach to updating markov-based models for predicting pavement performance. *Transportation Research Record: Journal of the Transportation Research Board*, 2366, 34–42. doi:10.3141/2366-04.
- Thube, D.T., 2012. Artificial Neural Network (ANN) based pavement deterioration models for low volume roads in India. *International Journal of Pavement Research and Technology*, 5, 115–120.
- TRIP, 2016. *The interstate highway system turns 60: Challenges to its ability to continue to save lives, time and money*. Washington, DC. <https://www.infrastructureusa.org/the-interstate-highway-system-turns-60-challenges-to-its-ability-to-continue-to-save-lives-time-and-money/> [accessed 20 Feb 2020].
- Underwood, B.S., et al., 2017. Increased costs to US pavement infrastructure from future temperature rise. *Nature Climate Change*, 7, 704–707. doi:10.1038/nclimate3390.
- Von Quintus, H.L., Mallela, J., Bonaquist, R., Schwartz, C.W., and Carvalho, R.L., 2012. Calibration of rutting models for structural and mix design. *NCHRP Report*.
- Wang, D., et al., 2017. Influence of computation algorithm on the accuracy of rut depth measurement. *Journal of Traffic and Transportation Engineering (English Edition)*, 4, 156–164. doi:10.1016/j.jtte.2017.03.001.
- Wang, Z., et al., 2021. Prediction of highway asphalt pavement performance based on Markov chain and artificial neural network approach. *The Journal of Supercomputing*, 77, 1354–1376. doi:10.1007/s11227-020-03329-4.
- White, T.D., NCHR Program, A.A. of S.H. and T. Officials, N.R.C. (U. S.). T.R. Board, 2002. *Contributions of pavement structural layers to rutting of hot mix asphalt pavements*. National Academy Press. <https://books.google.com.lb/books?id=4ysP-dp-QPAC>.
- Wolters, A.S., and Zimmerman, K.A., 2010. Current practices in pavement performance modeling.
- Xiong, H., et al., 2012. A compromise programming model for highway maintenance resources allocation problem. *Mathematical Problems in Engineering*, 2012, 1. doi:10.1155/2012/178651.
- Yamany, Mohamed S., and Abraham, Dulcy M., 2021. Hybrid approach to incorporate preventive maintenance effectiveness into probabilistic pavement performance models. *Journal of Transportation Engineering, Part B: Pavements*, 147, 04020077. doi:10.1061/JPEODX.0000227.
- Yang, J., et al., 2003. Overall pavement condition forecasting using neural networks—an application to florida highway network. In: *82nd Annu. Meet. Transp. Res. Board*.
- Yao, L., et al., 2019. Establishment of prediction models of asphalt pavement performance based on a novel data calibration method and neural network. *Transportation Research Record*. doi:10.1177/0361198118822501.
- Zhang, Z., and Gao, L., 2018. A nested modelling approach to infrastructure performance characterisation. *International Journal of Pavement Engineering*, 19, 174–180. doi:10.1080/10298436.2016.1172712.
- Zhou, F., and Scullion, T., 2002. Discussion: three stages of permanent deformation curve and rutting model. *International Journal of Pavement Engineering*, 3, 251–260. doi:10.1080/1029843021000083676.
- Zimmerman, K.A., and Ram, P. V., 2015. Pavement management's role in an asset management world. In: *9th Int. Conf. Manag. Pavement Assets*.